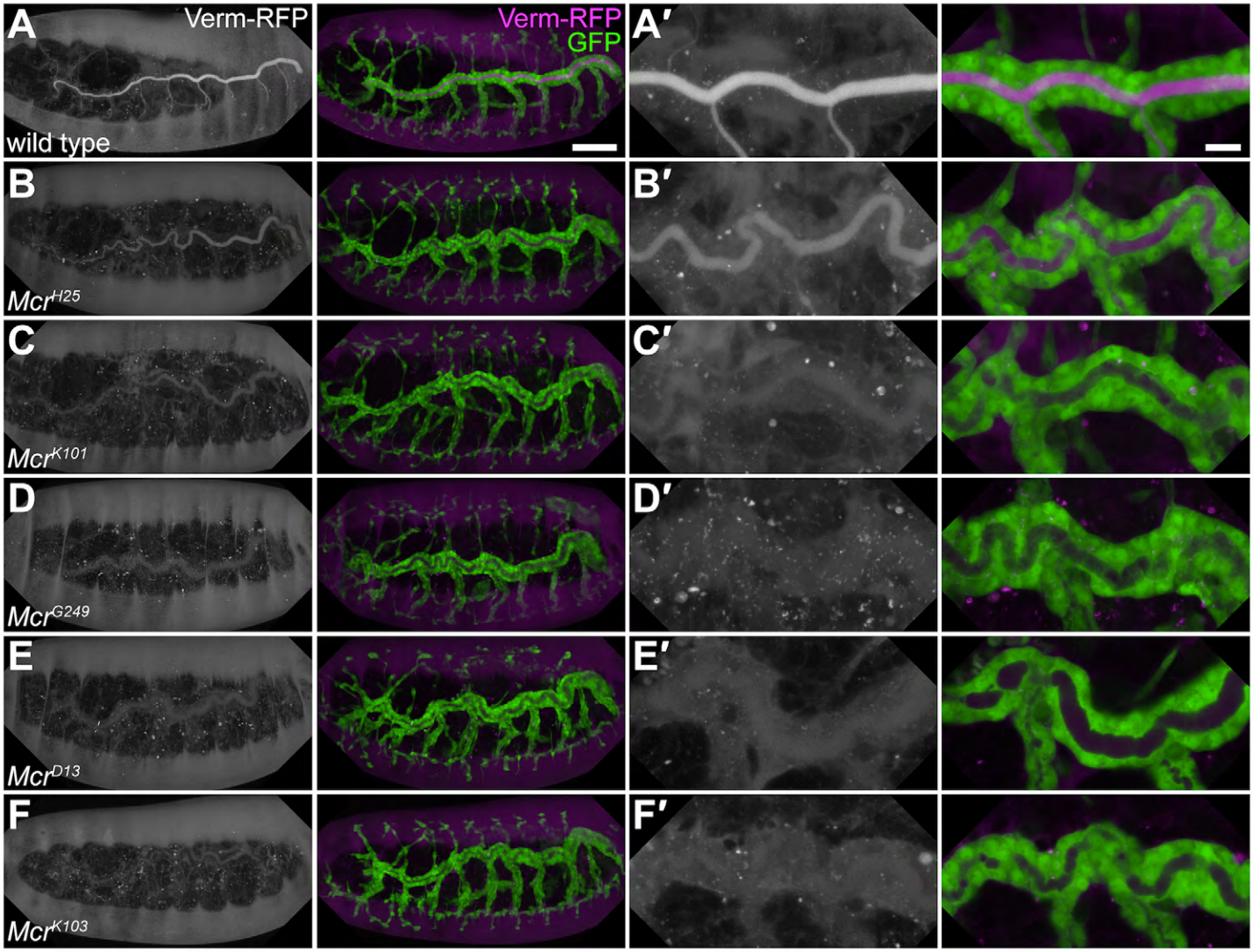

Supplemental Fig. 1. *Mcr* alleles show defects in tracheal tube size and luminal protein accumulation. (A-F) Confocal projections of living stage 15 embryos expressing GFP and Verm-RFP in tracheal cells controlled by *btl-Gal4*. All *Mcr* alleles show overelongated tracheae and impaired luminal accumulation of Verm-RFP. Mcr^{H25} is a hypomorphic allele, whereas Mcr^{K101}, Mcr^{G249}, Mcr^{D13}, and Mcr^{K103} are amorphic alleles showing comparable defects in tube elongation and Verm-RFP accumulation. (A′-F′) show close-ups of the tracheal DT of the embryos in (A-F). Scale bars: 50 µm (A-F), 10 µm (A′-F′)

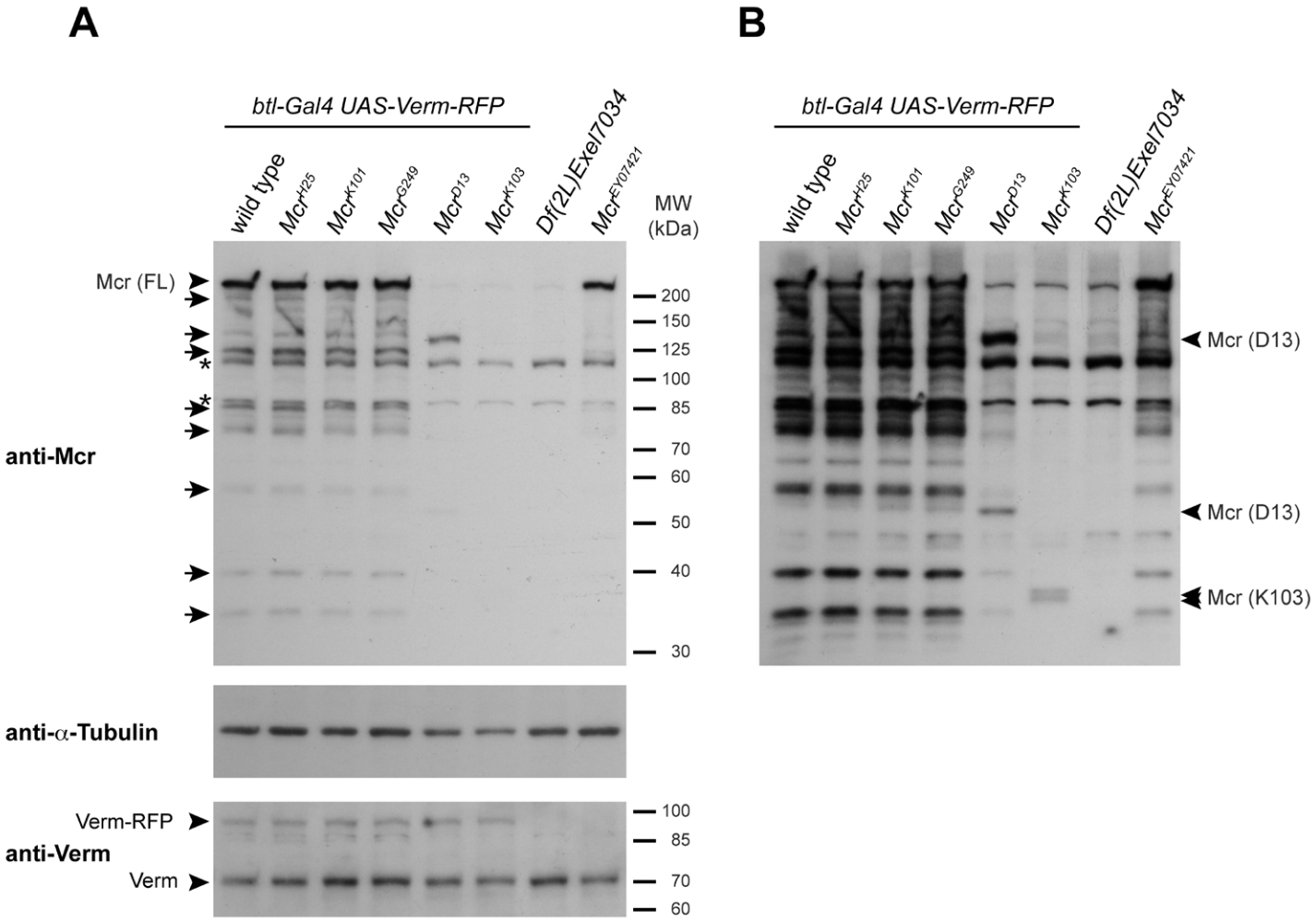

Supplemental Fig. 2. Characterization of Mcr protein in EMS-induced *Mcr* alleles. (A,B) Immunoblot of extracts from *Mcr* mutant embryos (14-17 hour AEL). A longer exposure of the immunoblot in (A) is shown in (B). Genotypes are indicated at the top. The amounts and apparent molecular weight of Mcr proteins in Mcr^{H25}, Mcr^{K101} and Mcr^{G249} mutant embryos are indistinguishable from Mcr in wild-type extracts. In contrast, full length Mcr (Mcr FL) is strongly reduced in extracts of Mcr^{D13}, Mcr^{K103} and *Df(2L)Exel7034* embryos. The residual Mcr FL band in these mutants presumably reflects perduring maternal wild-type Mcr protein. Mcr^{D13} shows two smaller bands of ~130 and 55 kDa, while Mcr^{K103} shows a doublet band at ~35 kDa (arrowheads in (B)). Note that the amounts of endogenous Vermiform (Verm) and transgenic Verm-RFP proteins are indistinguishable between *Mcr* mutants and wild-type controls, indicating that the reduced luminal levels of Verm-RFP observed in *Mcr* mutants are not due to lower Verm-RFP expression. Lower-MW bands, which may represent processed Mcr protein isoforms or degradation products, are indicated by arrows to the left in (A). Asterisks to the left in (A) indicate non-specific bands, which are also present in extracts from *Df(2L)Exel7034* embryos lacking the *Mcr* gene. Positions of a MW marker are indicated to the right in (A). A longer exposure of the same immunoblot (B) shows a double band of a truncated protein in Mcr^{K103} mutants at around 35 kDa and also an additional degradation band in Mcr^{D13} mutants. The wild-type and *Df(2L)Exel7034* lanes are the same as shown in supplementary material Fig. 3E.

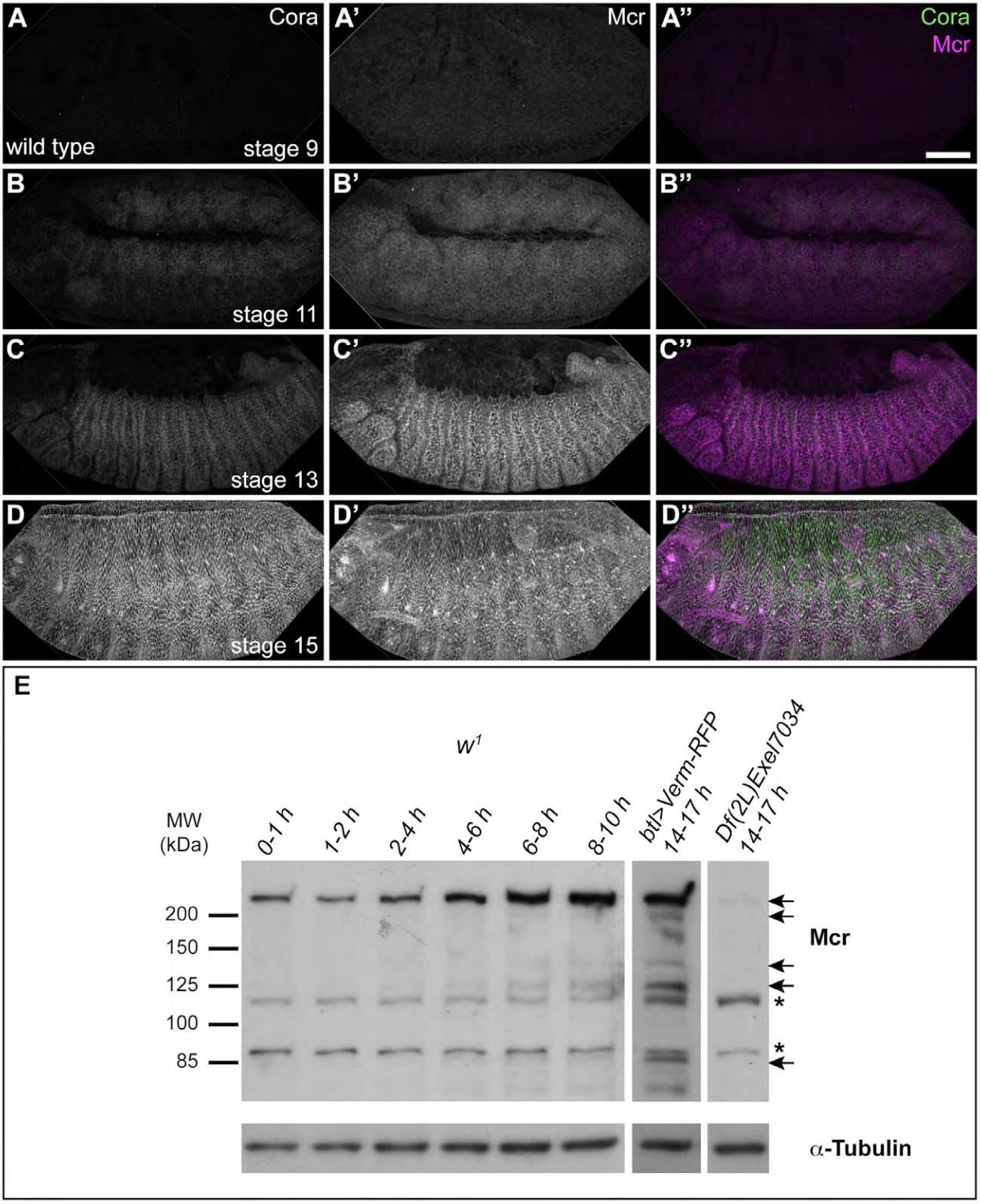

Supplemental Fig. 3. Time course of Mcr protein expression during embryogenesis. (A-D) Wild-type embryos were stained for Cora (A-D, green in A"-D") and Mcr (A′-D′, magenta in A"-D"). Embryonic stages are indicated. Note that Mcr starts earlier than Cora to accumulate at epidermal cell membranes. Scale bar: 50 µm. (E) Immunoblot against Mcr protein in embryonic extracts. Age and genotypes of embryos are indicated on top. Positions of a molecular weight (MW) marker are indicated to the left. Full length Mcr protein is detected at an apparent MW of above 200 kDa. Bands of lower MW (marked by arrows to the right) represent processed Mcr protein isoforms or degradation products. Asterisks mark non-specific bands, which are also detected in extracts from *Df(2L) Exel7034* embryos lacking the *Mcr* gene. The presence of full-length Mcr protein in 0-1h embryos presumably reflects maternally contributed Mcr. The faint band resembling the size of full-length Mcr in *Df(2L)Exel7034* embryos is presumably due to perduring maternal Mcr protein in the deficiency embryos. Note the increase in Mcr protein levels at 4-6 hour, which coincides with the appearance of zygotic *Mcr* transcripts detectable by *in situ* hybridization in embryos.

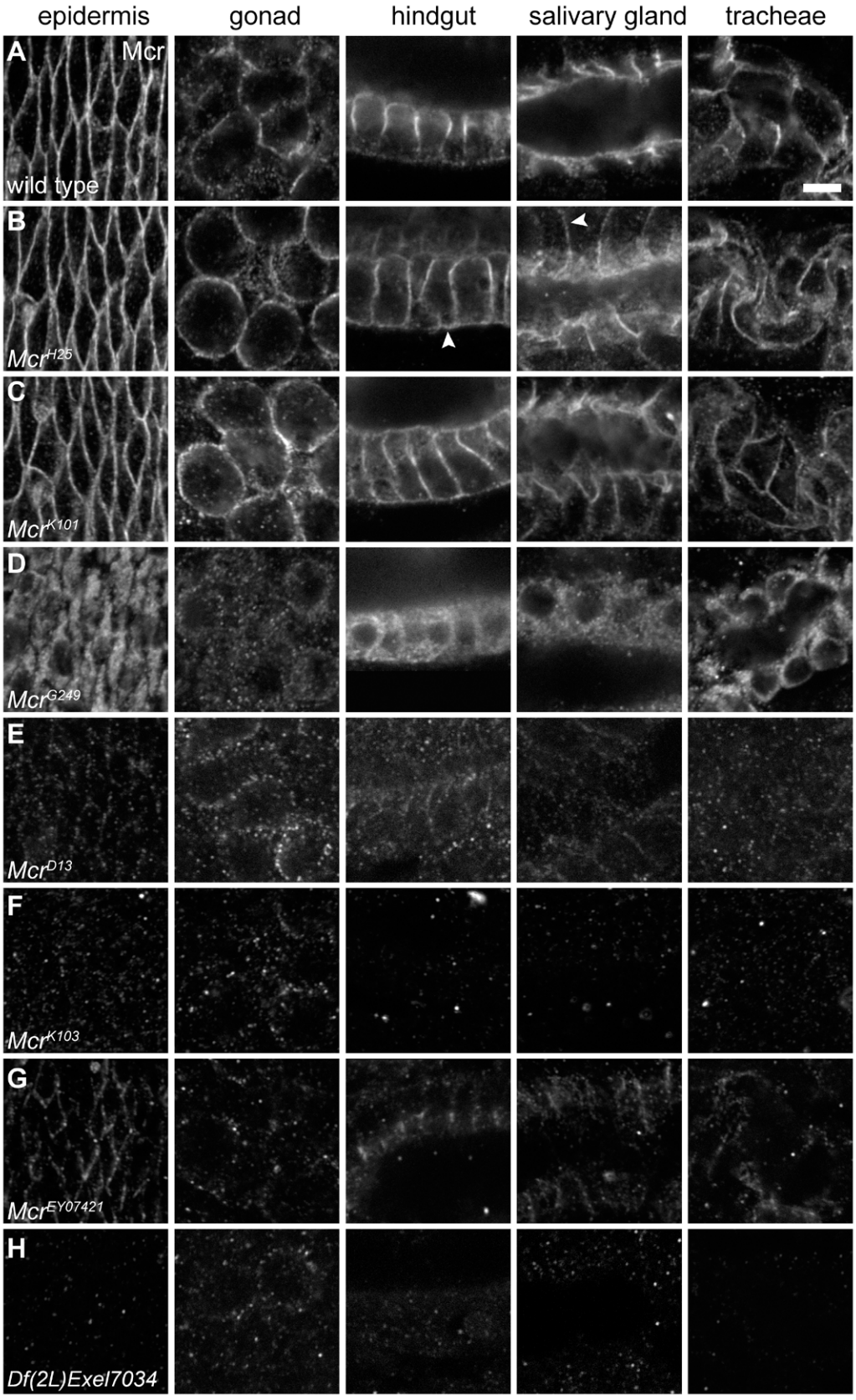

Supplemental Fig. 4. Subcellular localization of Mcr protein is altered in *Mcr* mutants. (A-H) Confocal sections of stage 16 embryos immunostained for Mcr protein. Close-ups of epidermis, gonads, hindgut, salivary glands, and tracheae are shown in wild-type embryos (A) and in the *Mcr* mutant alleles used in this study (B-H). In Mcr^{H25} (B) and Mcr^{K101} (C) mutants the distribution of Mcr protein extends towards the basal side of hindgut and salivary gland cells (arrowheads; apical is up). Mcr^{G249} (D) mutants show intracellular accumulation of Mcr protein. In Mcr^{D13} (E) only residual protein is detected in germ cells and the hindgut. Mcr signals are absent in Mcr^{K103} (F) embryos and strongly reduced in $Mcr^{EY07421}$ (G) embryos. *Df(2L)Exel7034* (H) embryos lack zygotic Mcr protein. Residual signals in germ cells of *Df(2L)Exel7034* embryos may represent perduring maternal Mcr protein. Scale bar: 5 µm.

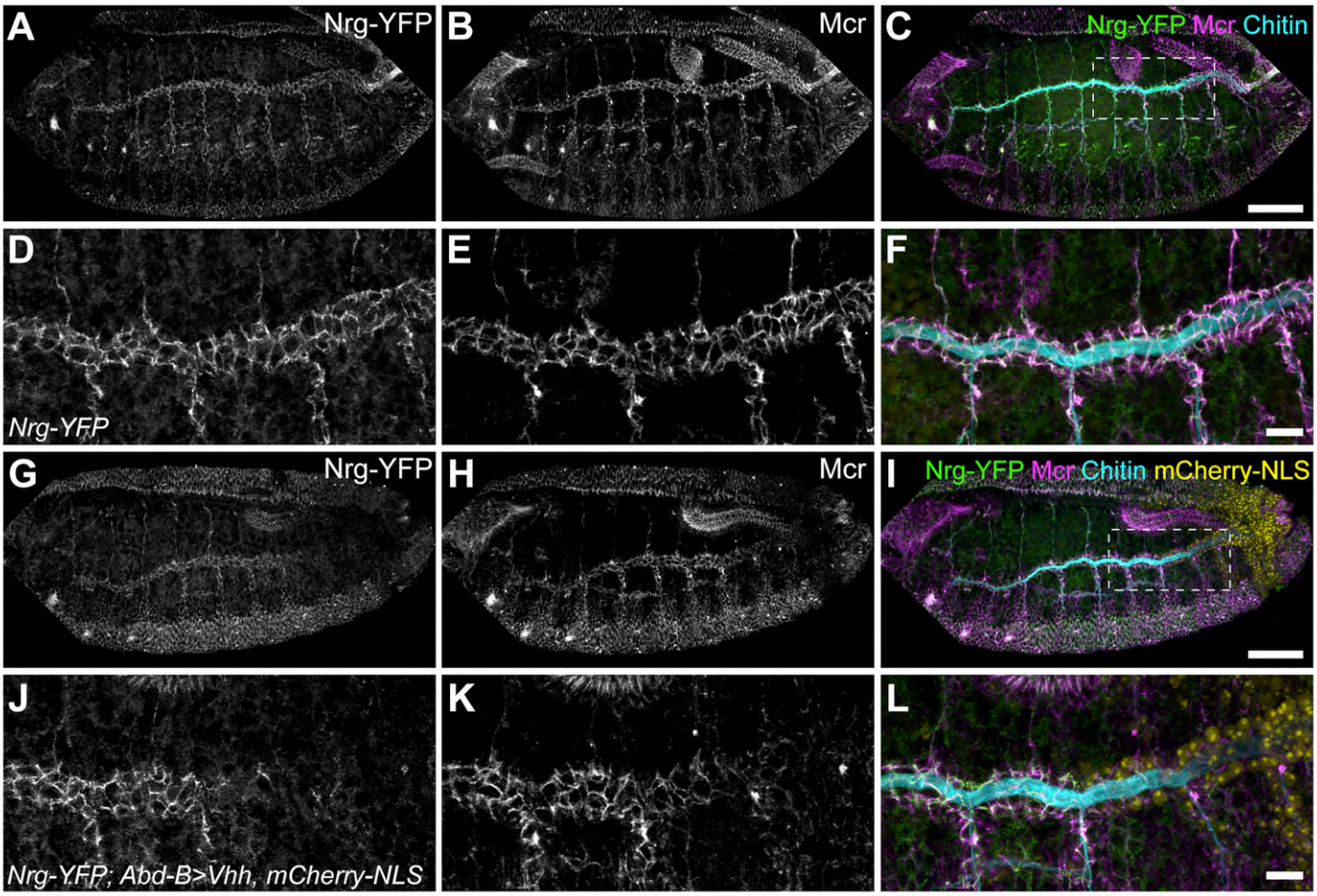

Supplemental Fig. 5. Mcr protein is lost upon anti-GFP nanobody-mediated degradation of Nrg. (A-L) Male stage 15 embryos hemizygous for a YFP protein trap in the *Nrg* locus (Nrg-YFP) were stained for YFP (A,D,G,J; green in C,F,I,L) and Mcr (B,E,H,K; magenta in C,F,I,L). Chitin is labeled in cyan. (D-F) and (J-L) are close-ups of the boxed regions marked in (C) and (I), respectively. (A-F) show a control embryo, in which Nrg-YFP and Mcr colocalize at lateral cell membranes in tracheal and other epithelial cells. In (G-L) expression of anti-GFP nanobodies coupled to the F-Box protein Slmb was driven by *Abd-B-Gal4* (*Abd-B >Vhh*) in the posterior body segments. The nanobody-expressing cells are labeled by co-expression of mCherry-nls (yellow in I,L). Note that Nrg-YFP levels are reduced in the cells expressing the anti-GFP nanobody (J,L). Mcr is depleted from the membrane of the nanobody-expressing cells (K). The control embryo in (A-F) does not express *Abd-B-Gal4*. Scale bars: 50 µm (A-C,G-I), 10 µm (D-F,J-L).